Mathematical Biology

Seidel–Herzel model of human baroreflex in cardiorespiratory system with stochastic delays

Aleksandra Dudkowska · Danuta Makowiec

Abstract The stochastic versus deterministic solution of the Seidel–Herzel model describing the baroreceptor control loop (which regulates the short-time heart rate) are compared with the aim of exploring the heart rate variability. The deterministic model solutions are known to bifurcate from the stable to sustained oscillatory solutions if time delays in transfer of signals by sympathetic nervous system to the heart and vasculature are changed. Oscillations in the heart rate and blood pressure are physiologically crucial since they are recognized as Mayer waves. We test the role of delays of the sympathetic stimulation in reconstruction of the known features of the heart rate. It appears that realistic histograms and return plots are attainable if sympathetic time delays are stochastically perturbed, namely, we consider a perturbation by a white noise. Moreover, in the case of stochastic model the bifurcation points vanish and Mayer oscillations in heart period and blood pressure are observed for whole considered space of sympathetic time delays.

1 Introduction

Complex rhythmic processes are typical for living organisms [1]. The human cardiovascular system is a paradigmatic source of the fundamental physiological rhythm—the heart rate, and is controlled by several neural and hormonal mechanisms. Blood pressure and electrocardiogram (ECG) are the easiest signals to measure from the

A. Dudkowska (✉) · D. Makowiec
Institute of Theoretical Physics and Astrophysics, University of Gdańsk ul,
Wita Stwosza 57, 80-952 Gdańsk, Poland
e-mail: ola@iftia9.univ.gda.pl

cardiovascular system. The continuous ECG can be transformed into a discrete signal of normal beat-to-beat cardiac periods, called NN-intervals. It has been demonstrated that NN-intervals fluctuate in a complex manner: they show the long-range temporal autocorrelations [2,3], multifractal scaling properties [4,5], and share characteristics of a physical system in a critical state [6].

The variation in NN series is termed heart rate variability (HRV). It has been shown that HRV represents the most promising marker in recognizing the relationship between the autonomic nervous system and the cardiovascular mortality [7–9]. The heart rate can be increased by slowly acting sympathetic activity or decreased by fast acting parasympathetic (vagal) activity. The balance between the effects of sympathetic and parasympathetic nervous systems—the two parts of the autonomic nervous system, is believed to be reflected in the beat-to-beat changes of the fundamental cardiac cycle.

Respiratory sinus arrhythmia (RSA) is the name of the heart rate modulation due to the parasympathetic activity which is related to the respiratory cycle. RSA is characterized by the frequency around 0.25 Hz.

The source of frequency oscillations about 0.1 Hz present in the heart rate and the blood pressure (so-called Mayer waves) is still debated on (see [9,10] for discussion and references). The most accepted theory suggests that these waves are caused by the delayed feedback control of the blood pressure through baroreflex. In general, physiological role of baroreflex is to monitor and regulate the blood pressure and ultimately maintain circulation to brain and other organs [11]. There are strong clinical links between the sympathetic activity and the Mayer waves—if sympathetic activity is chemically blocked, Mayer waves are significantly reduced or completely eliminated [12].

The NN interval series are the source of information about the underlying mechanisms behind the human cardiovascular system. Recently, the concept of synchronization has been exploited for the purpose of identifying the interdependencies between coupled subsystems. Synchronization phenomenon is a process of adjustment of oscillators due to mutual interactions, see [13] for an introduction. Although the interaction between the respiratory and the cardiac rhythm is rather weak, the synchronization between these rhythms has been demonstrated [14–21]. However, in order to verify and analyze the synchronization of this sort, there is a need of accessing to the system's parameters [22], and hence the corresponding models are required.

Living systems are becoming increasingly accessible to modeling. The so-called open loop conditions, where parts of the control system are studied in isolation, contributed to a better understanding of the physiology of cardiac control. A vast number of mathematical models of short-term pressure control system has emerged as the result of this approach. The other approach for modeling is by recovering nonlinear dynamics directly from the time series [23,24]. The fundamental hypothesis underlying mathematical modeling of HRV is that the changes in the cardiac rhythm can be associated with bifurcations in the model [1]. Bifurcations in a real-life system can be understood as, for instance, shifting the unhealthy rhythms into the normal one due to applied drugs.

A popular model for HRV was proposed by DeBoer et al. [25]. In this model the blood pressure, respiration, peripheral resistance and the cardiac interbeat intervals are represented by a simple beat-to-beat relations. Within this model the oscillations similar to Mayer waves appear due to the delay in the sympathetic control loop of

the baroreflex. Abbiw–Jackson et al. [26] proposed a model in which the main factor leading to oscillations is the increase of baroreflex feedback amplitudes (gains). Eyal et al. [27] studied simplified linearized version of DeBoer model. They found that the increase of sympathetic gain or the decrease of vagal gain parameters leads via Hopf bifurcation to sustained oscillations. Ottesen [28] modeled chronotropic (heart rate regulation) and inotropic (contractility of ventricle regulation) parts of the baroreflex-feedback mechanism. The system can switch between being stable and oscillatory following the changes in the sympathetic time delay. The role of delays times and gains within the extension of the Ottesen model was investigated by Fowler et al. to explain the relation between decreasing gains and aging [29]. In the model proposed by Ursino et al. [30] the combination of increases in gains and delays is required to induce instability.

The idea of Seidel and Herzel proposition (SH model), is based on including the internal dynamics of one heartbeat [31]. It is achieved by introducing a phase of the sinus node (the first pacemaker of the heart) and then considering the sensitivity of the sinus node phase change to the autonomic neurotransmitter kinetics and the vascular dynamics. An increase of the delays in conveying of sympathetic nervous system signals leads via Hopf bifurcation to the heart rate oscillations [32]. These oscillations are interpreted as Mayer waves. Recently this approach was used in modeling the complex phenomena related to heart dynamics, such as synchronization between the respiration and the heart rate [33] or the presence of $1/f$ fluctuations in the interbeat interval signals. Also some autonomic nervous system dysfunctions were simulated by manipulation of the parameters of SH model [34].

It is known that the cardiovascular signals behave deterministically, but the noise of various origins is one of their inherent properties [1,35,36]. The basic neurotransmitter of the sympathetic nervous system—noradrenaline, is distributed to the heart and vessels via the diffusion. Therefore this process should be represented by a slow dynamics dependent on a stochastic process. Moreover, sympathetic time delays play a special role in the system—they are the bifurcation parameters. Depending on the delays values the SH model solution can be a fixed point or can exhibit sustained oscillations. Therefore it is interesting how the solution changes if stochastically driven delays in signal transfer are considered—this is the central aim of the present work. We demonstrate that the heartbeat intervals—solutions of SH model with stochastic delays provide NN series with PDFs that are closer to real-life series and exhibit low frequency modulations (Mayer waves) independently of the mean values of delays. We focus our interest on the bifurcation regime. This regime demands careful dealing with model parameters. For that reason we present and discuss the basic model in detail.

We start with the introducing of HRV measures (Sect. 2), then we present the SH model (Sect. 3). We give also the basic underlying physiological reasoning behind the mathematical relations. In Sect. 4 we show the solution obtained for the representative parameter settings and discuss the influence of the presence of respiratory oscillations. Next, we present the stability diagrams obtained when the delays in the transmission of sympathetic activity change (Sect. 5), and finally, in Sect. 6 we observe the changes that occur when the delays are perturbed by a noise.

2 The HRV analysis

Before we move on to the theoretical study, we want to present the methods of HRV analysis, which we use in order to compare numerical results to the real-life NN data. HRV can be analyzed in different ways [7]: time domain, frequency domain and nonlinear methods are used. One of them (within the so-called geometrical methods of the time domain) converts NN intervals into the sample probability distribution function (PDF) of NN intervals. Then for example, the width of the histogram at a specific height is converted into the measure of HRV or/and its geometric shape is classified into several pattern-base categories (e.g., triangular-like shape is used in clinical practice).

The nonlinear method of HRV analysis applied in this paper is the Poincaré plot. It is a diagram in which each NN interval is plotted as a function of the previous one. A plot of this sort provides a graphical presentation of the correlation between consecutive RR intervals. Woo [37] classified qualitatively shapes of Poincaré plot of RR series, which characterize the degree of the signal complexity.

The real physiological data were collected and prepared in the Medical Academy of Gdańsk [38]. For each person the 24-hour ECG Holter monitoring was performed. The 24-h ECG Holter signals are annotated to extract normal RR signals. The group chosen to analyze consists of 15 healthy individuals without a history of any cardiovascular disease, with both echocardiogram and electrocardiogram in the normal range. The left ventricle ejection fraction was normal. From each signal the 5-h continuous diurnal subset was extracted in order to obtain a stationary series.

The exemplary histograms obtained for the real-life data are presented in Fig. 1, and the Poincaré plots in Fig. 2.

3 SH model

SH model provides empirical relations between different mechanisms involved in the baroreceptor-cardiac reflex. The arguments behind these relations are strongly physiologically grounded; [32] brings a detailed discussion. It could be instructive to learn about modeling of the physiology of the human cardiovascular control system from [32,28], here however we present a simplified summary to give the background for understanding the role played by parameters in the considered model. For a systematic description of the cardiovascular system and its control we refer to [8–10] and references therein.

The arterial baroreflex can be considered to be a feedback control system because it maintains mean arterial pressure near the target value using the set of sensors and effectors, see Fig. 3 for the visualization of relationships between the variables. The sensors are arterial baroreceptors—nerve fiber endings in arterial walls, which are sensitive to the arterial blood pressure. The rate at which the blood pressure changes:

— baroreceptor activity v_b:

$$v_b = k_1(p - p^{(0)}) + k_2 \frac{dp}{dt} \tag{1}$$
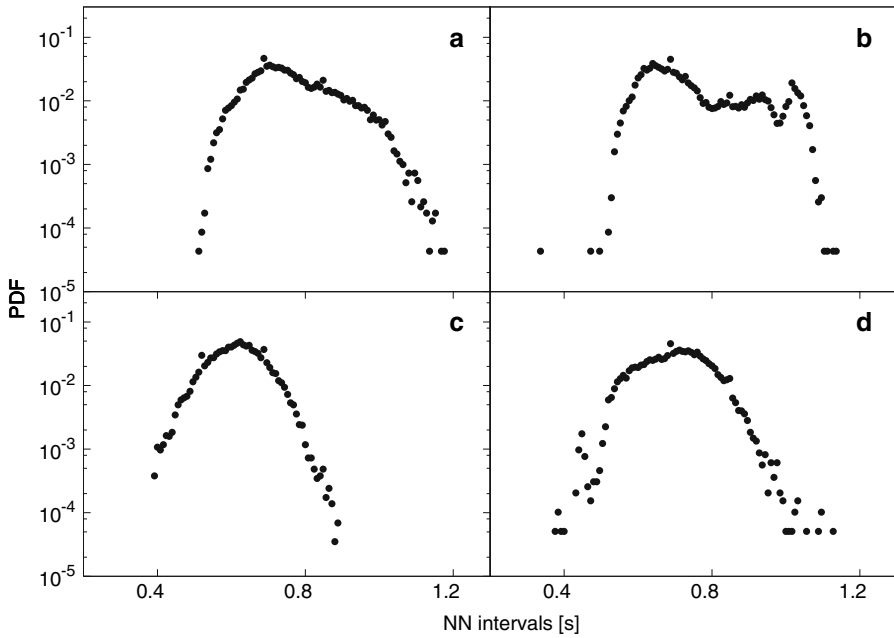
Fig. 1 The examples of probability density functions (*PDF*) of the NN series obtained for healthy subjects during daily activity. See text for detailed description of the data. The bin of the histogram is equal to 8 ms, the log scale is applied to the PDF axis
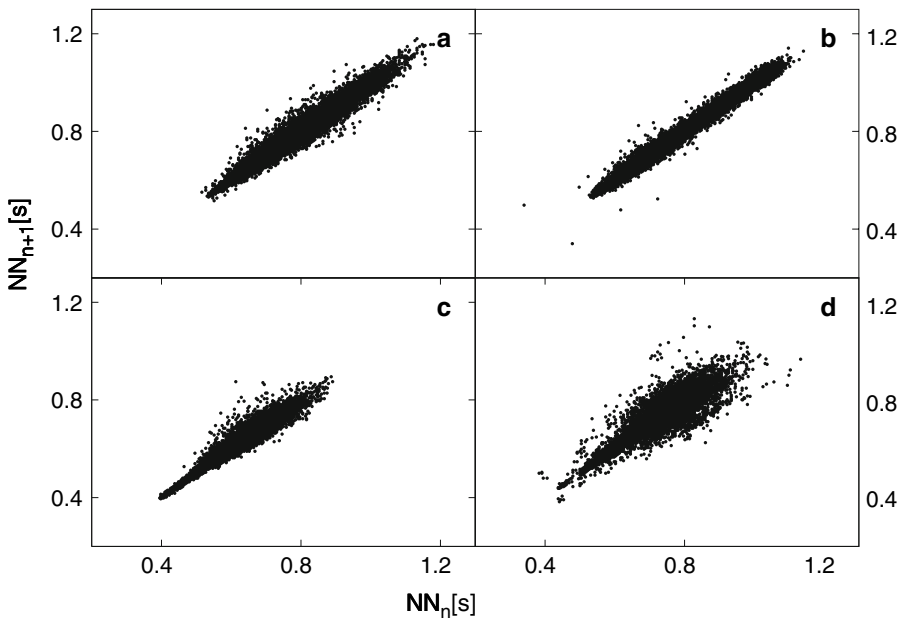
Fig. 2 Examples of Poincaré plot for the same healthy subjects as in Fig. 1
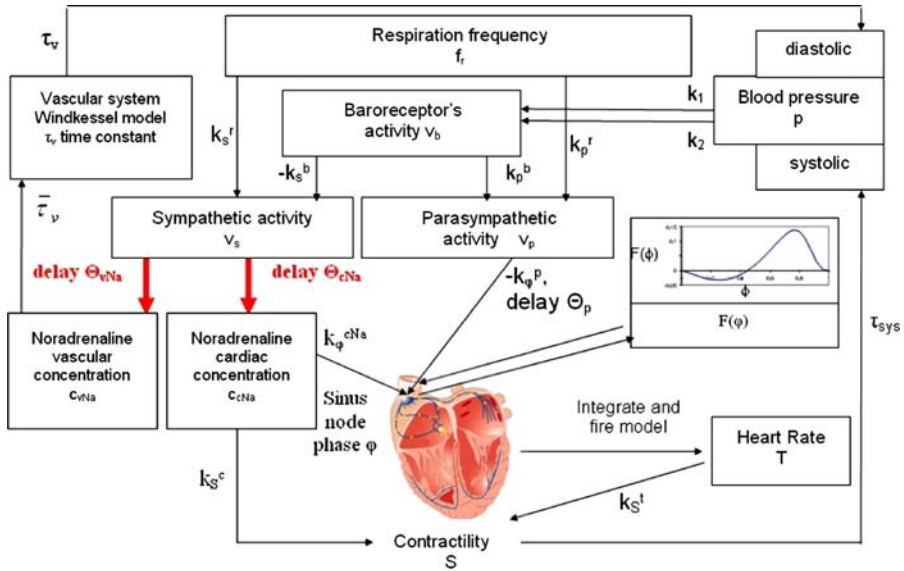
Fig. 3 The scheme of SH model of the baroreceptor control loop. *Arrows* depict relations between variables

(p—blood pressure; $k_1 = 0.02$ mmHg^{-1}, $k_2 = 0.00125$ s mmHg^{-1}, $p^{(0)} = 50$ mmHg—parameters)

When blood pressure rises the baroreceptors fire more signals into the medulla in the brain. Usually the medulla responds by sending signals along the sympathetic system (an inhibiting signal) and the parasympathetic system (an activating signal). Moreover, the activity of both subsystems is modulated by respiration:

— sympathetic activity v_s:

$$v_s = \max(0, v_s^{(0)} - k_s^b v_b + k_s^r |\sin(\pi f_r t + \Delta\phi_s^r)|) \qquad (2)$$

($f_r = 0.2 s^{-1}$—respiratory frequency; $v_s^{(0)} = 0.8$, $k_s^b = 0.7$, $k_s^r = 0.1$, $\Delta\phi_s^r = 0.0$—parameters)

— parasympathetic activity v_p:

$$v_p = \max(0, v_p^{(0)} + k_p^b v_b + k_p^r |\sin(\pi f_r t + \Delta\phi_p^r)|) \qquad (3)$$

(f_r—respiratory frequency; $v_p^{(0)} = 0.0$, $k_p^b = 0.3$, $k_p^r = 0.1$, $\Delta\phi_p^r = 0.0$—parameters)

The parasympathetic system is relatively fast-acting, the heart rate is generally reduced within a time interval smaller than the time between the heart beats. Conversely, the heart rate increases in response to the sympathetic signals via much slower action—the diffusion of chemicals noradrenaline (Na) called also norepinephrine.

There are delays of 2–5 s before the sympathetic impulse takes effect in changing the cardiac concentration of Na:

— cardiac concentration of sympathetic transmitter c_{cNa}:

$$\frac{dc_{cNa}}{dt} = -\frac{c_{cNa}}{\tau_{cNa}} + k^s_{c_{cNa}} v_s(t - \theta_{cNa})$$ (4)

($\tau_{cNa} = 2.0s$, $k^s_{c_{cNa}} = 1.2$—parameters, θ_{cNa}—time delay)

In the absence of the feedback from the autonomic nervous system the heart is known to continue beating spontaneously at a rate set by firing of the sino-atrial node. This intrinsically controlled behavior is described in the model by the idea of the sinus node phase ϕ.

In the absence of the baroreflex control the phase is assumed to grow linearly up to the threshold value 1 after which abruptly switches to 0 (integrate-and-fire model) [39]. Hence, a heart beat is generated each time the phase is reset to 0. The heart rate is raised following the increase in the concentration of Na and conversely is reduced with the increase of the vagal activity. In addition, the action of the vagal system to the heart rate depends on the phase of the heart cycle. To simulate this dependence a concept of a phase-effectiveness curve is introduced:

— phase effectiveness curve F:

$$F(\varphi) = \varphi^{1.3}(\varphi - 0.45)\frac{(1 - \varphi)^3}{(1 - 0.8)^3 + (1 - \varphi)^3}$$ (5)

Moreover the saturation property of a physiological signal $x(t)$ is simulated by a sigmoidal function as follows:

$$x(t) \longrightarrow_{x_0, y_0} \widetilde{x}\,[x(t); x_0, y_0] = x(t) + (x_0 - x(t))\frac{x(t)^{y_0}}{x_0^{y_0} + x(t)^{y_0}}$$ (6)

where x_0, y_0 are parameters which are characteristic for a given signal saturation.

Then the change of the sinus node phase is modeled as follows:

— sinus node phase φ:

$$\frac{d\varphi}{dt} = \frac{1}{T^{(0)}} f_s(t) f_p(t)$$ (7)

(f_s, f_p—sympathetic and parasympathetic influences; $T^{(0)} = 1.1$ s—parameter)

— sympathetic influence on the phase velocity of the sinus node:

$$f_s(t) = 1 + k^{cNa}_\varphi \widetilde{c_{cNa}}[c_{cNa}(t); \widehat{c}_{cNa}, n_{cNa}]$$ (8)

($k^{cNa}_\varphi = 1.6$, $\widehat{c}_{cNa} = 2.0$, $n_{cNa} = 2.0$—parameters)

— parasympathetic influence on the phase velocity of the sinus node:

$$f_p = 1 - k_\varphi^p \tilde{v}_p[v_p(t - \theta_p); \widehat{v}_p, n_p]F(\varphi) \tag{9}$$

($v_p(t-\theta_p)$—delayed parasympathetic activity, $F(\varphi)$—phase effectiveness curve, $k_\varphi^p = 5.8, \widehat{v}_p = 2.5, n_p = 2.0$—parameters)

The cardiac concentration of Na influences the heart contractility—the strength with which the blood is pumped into vessels:

— cardiac contractility S_i':

$$S_i' = S^{(0)} + k_S^c c_{cNa} + k_S^t T_{i-1} \tag{10}$$

(T_{i-1}—duration of the previous heart period; $S^{(0)} = 25\,\text{mmHg}, k_S^c = 40\,\text{mmHg}, k_S^t = 10\,\text{mmHgs}^{-1}$—parameters) then saturated:

$$S_i = \widetilde{S}_i'[S_i'(t); \widehat{S}, n_S] \tag{11}$$

($\widehat{S} = 70$ mmHg, $n_S = 2.5$: parameters)

Arteries and capillaries resistance to flow is increased by the sympathetic activity signals when signal rate increases. The vascular system is modeled by the Windkessel model. The blood pressure decay during the diastole, described by the Windkessel time constant, is modulated by the vascular noradrenaline concentration, which follows sympathetic activity. Thus, the sympathetic activity enters the system via two ways: directly to the heart and to the vessels. Each impact is delayed with its characteristics:

— Windkessel time constant τ_v:

$$\tau_v = \tau_v^{(0)} - \overline{\tau_v} \widetilde{c_{vNa}}[c_{vNa}(t); \widehat{c}_{vNa}, n_{vNa}] \tag{12}$$

($\tau_v^{(0)} = 2.2s, \overline{\tau_v} = 1.2s, \widehat{c}_{vNa} = 10.0, n_{vNa} = 1.5$—parameters)

— vascular concentration of sympathetic transmitter c_{vNa}:

$$\frac{dc_{vNa}}{dt} = -\frac{c_{vNa}}{\tau_{vNa}} + k_{c_{vNa}}^s v_s(t - \theta_{vNa}) \tag{13}$$

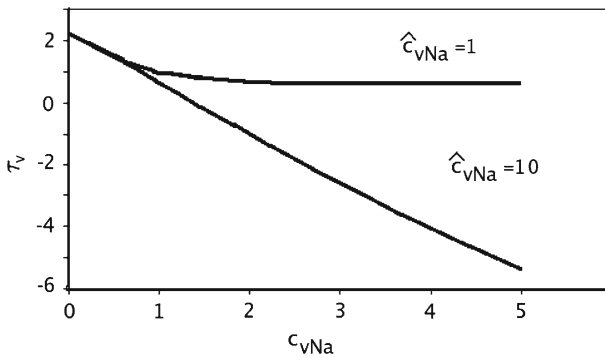($\tau_{vNa} = 2.0s, k_{c_{vNa}}^s = 1.2$—parameters, θ_{vNa}—time delay)

Finally, the loop is closed by setting the changes in blood pressure:

— blood pressure during the systolic part of the heart cycle:

$$p = d_{i-1} + S_i \frac{t - t_i}{\tau_{sys}} exp \left\{ 1 - \frac{t - t_i}{\tau_{sys}} \right\} \tag{14}$$

(d_{i-1}—diastolic pressure during the systolic part of the heart cycle, t_i—time of last contraction onset, $\tau_{sys} = 0.125$ s—parameter)

Fig. 4 The dependence of τ_v on c_{vNa}: the case when $\widehat{c}_{vNa} = 10.0$ and $\widehat{c}_{vNa} = 1.0$

— blood pressure during the diastolic part of the heart cycle:

$$\frac{dp}{dt} = -\frac{p}{\tau_v(t)} \tag{15}$$

SH model modification:

(a) Figure 4 presents the dependence of τ_v—Windkessel time 'constant' on c_{vNa}, which follows Eq. (12). Such dependence leads to negative τ_v. However, since τ_v is responsible for the blood pressure decay in aorta during diastolic part of the heartbeat cycle, see Eq. (15), it must be positive. Based on this we propose the following change in the sigmoidal function parameter: let $\widehat{c}_{vNa} = 1.0$ in place of $\widehat{c}_{vNa} = 10.0$. This change becomes important only in the case when delays θ_{cNa}, θ_{vNa} are greater than 3.0. The similar change was introduced in [34].

(b) Kotani et al. [33] modified the model to incorporate the baroreflex impact to the respiratory synchronization and back to study the cardiorespiratory synchronization.

(c) The phase effectiveness curve $F(\varphi)$ replaced by a constant was considered in [31,34]. It has been observed that this change critically influences the stability of the solution with respect to the coupling between baroreceptors and vagal nerves [31].

4 Numerical simulation of the model

The adapted Runge–Kutta method of fourth order with a constant step size ($h = 0.001$ s) [40] is used. The ring buffers are introduced to store the history of sympathetic and vagal activities. The first 500 s of the evolution are neglected as a transient time. Then results are collected and analyzed. The results with parameters setting as in the original Seidel–Herzel proposition are presented in Fig. 5. Subsequently, starting from the top of Fig. 5, we show: (left panel with respiratory included, right panel without respiratory)

– The blood pressure p which is characterized by a rapid increase during the systole, and a gentle decrease during the diastole. Minimum (diastolic—about 80 mmHg)
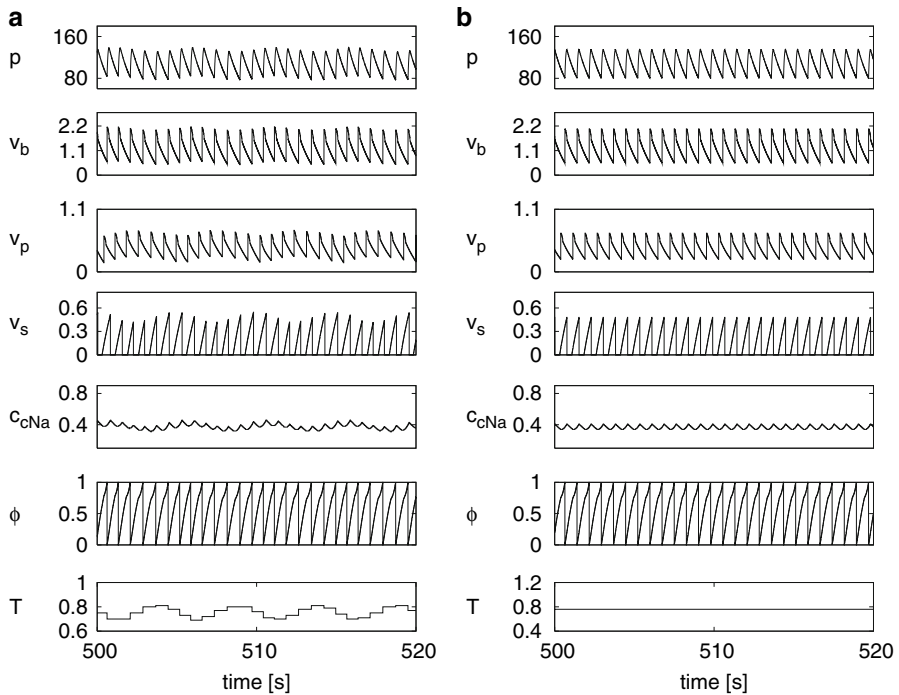
Fig. 5 Time series of the SH model basic variables: blood pressure $p(t)$ (mmHg), baroreceptor activity $v_b(t)$, parasympathetic activity $v_p(t - \theta_p)$, cardiac sympathetic activity $v_s(t - \theta_{cNa})$, concentration of Na in the heart $c_{cNa}(t)$, phase of sinus node $\phi(t)$ and the length of heart beat periods $T(t)$ (s). Time delays of sympathetic activity are constant and equal to each other $\Theta_{cNa} = \Theta_{vNa} = 1.65$s (**a**). The influence of respiration can be seen in modulations of waveforms (RSA) (**b**). Time series when the respiratory modulation of neural activities is neglected

and maximum (systolic—about 140 mmHg) values of this wave neatly reproduce the physiological data.

– Baroreceptors activity v_b is basically proportional to the blood pressure p. Hence the waves in the first and the second panels are similar.

– The parasympathetic activity v_p that affects the heart with a time delay θ_p is shown. Due to this delay the oscillations of the activity are shifted in time. Since transmission of the signal is fast, the delay can be assumed to be constant and relatively small, i.e., $\theta_p = 0.5$ s.

– The sympathetic system activity v_s enters in the model with two delays: θ_{cNa} and θ_{vNa} corresponding to its influence on the heart and vascular system, respectively. Delays $\theta_{cNa}, \theta_{vNa}$ represent the time intervals needed for the transmitters to transfer the information by diffusion. The activity affecting the heart $v_s(t - \theta_{cNA})$ is presented in the figure.

– The cardiac c_{cNa} and the vascular c_{vNa} Na concentrations take the same values if the delays θ_{cNa} and θ_{vNa} are identical.

– The phase of the sinus node φ is plotted. This phase mimics heart beating (integrate-and-fire model) and establishes the rhythm of the whole system. The intrinsic sinus
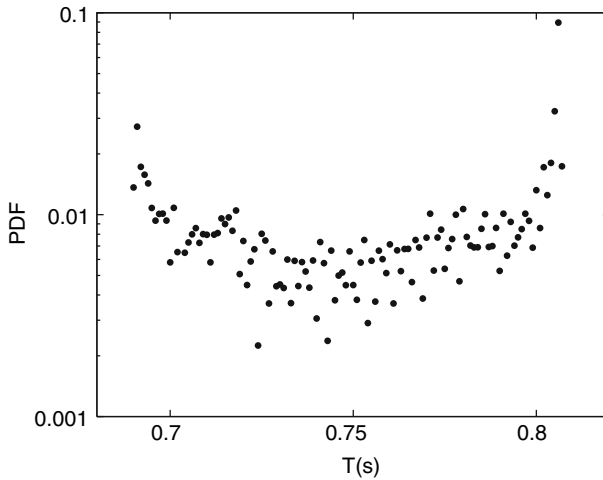
Fig. 6 PDF of time series *T(t)* presented on Fig.5a. The histogram bin is 0.001 s and the log scale to probability axis is applied. Time delays of sympathetic activity are constant and equal to each other $\Theta_{cNa} = \Theta_{vNa} = 1.65$s

node period is $T_0 = 1.1$ s but all variables of the model oscillate with a period about 0.8 s.

– The sequence of heart beat periods T_i, i.e., the time intervals between two consecutive heart beats are presented.

Our numerical results are slightly different from the results presented in [31]. To explain the difference let us observe that there is some inconsistency in the results of [31]. For example, assuming that the baroreceptor activity v_b takes values in the interval [1, 2.6] as it is shown in [31], then following Eq. (3) the parasympathetic activity v_p should vary in the interval [0.4, 0.9], hence it cannot exceed 1 which is what appears in Fig. 4 of [31].

The sympathetic and parasympathetic activities are influenced by the respiratory neurons. This relation is represented by the sine function in Eqs. (2) and (3). The blood pressure and heart period variation caused by the respiratory (RSA) is clearly visible in the plots of Fig. 5a.

All system variables are modulated with the frequency of respiration desirable. But the probability density function obtained from 2,500 beat-to-beat intervals shows, see Fig. 6, that the extremal values for heart periods—the minimal about 0.68 s and the maximal about 0.81 s, occur with a sharply peaked probability ten times larger than the mean value. Hence, the respiratory modulation provides the HRV which is far from properties of the real-life heart rate, see Fig. 1. RSA vanishes when the sine function is replaced by its average value and hence the respiratory modulation of the neural activities is neglected, see Fig. 5b. In our further simulations we concentrate on interactions other than those between the heart and respiration.

5 Stability in SH model due to time delays

It is well known that a control system which exhibits powerful responses and contains
time delays can be unstable that means it can cause the oscillations of variables which
grow in an unbounded fashion [41,42]. Such unstable control system can nevertheless
produce sustained, constant amplitude oscillation if the feedback control contains the
nonlinear elements that limit the swing of the variables.

The occurrence of the sustained oscillation in the SH model solution depends on
the values of the delays representing the transfer time of sympathetic activity to the
heart θ_{cNa} and to the vasculature θ_{vNa}. The sustained oscillation with a significant
large amplitude emerges in the SH model solution for certain pairs of $(\theta_{cNa}, \theta_{vNa})$.
For other values of $(\theta_{cNa}, \theta_{vNa})$, it occurs that series of T_i oscillate with the frequency
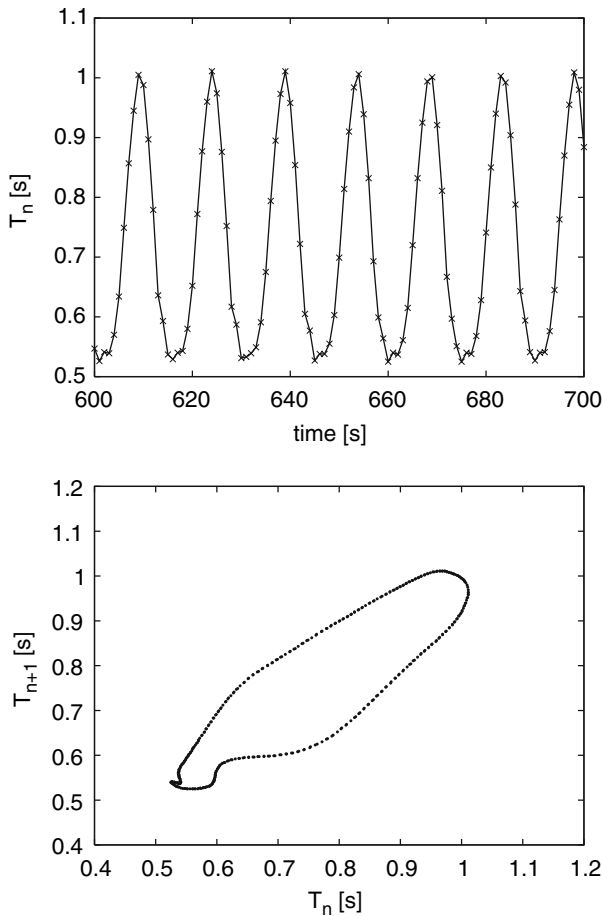
Fig. 7 The sustained oscillation solution in case when both delays are equal to $\Theta_{cNa} = \Theta_{vNa} = 3$ s. The
consecutive heart periods are not equal but oscillate with period ≈ 15 beats (*upper figure*). The attractor of
the system is the limit cycle consisting of 474 beats (*bottom figure*)
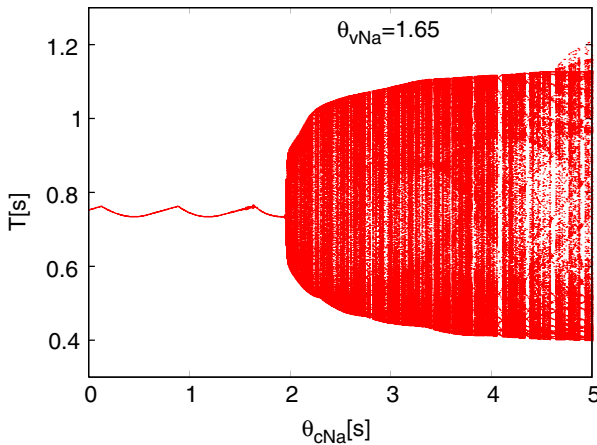
Fig. 8 Bifurcation diagram if the delay in transmitting signals from the brain to the heart θ_{cNa} is increasing, while the delay between the brain and the blood vessels is constant $\theta_{vNa} = 1.65$ s. The bifurcation transition shown here is considered in detail in the main text

about 0.1 Hz and the amplitude in the range of the integration step. To be precise, when the integration step h changes, the amplitude of the oscillation changes accordingly.

Let us define these two types of solution as:

– the fixed point solution: the heart rate is fixed. The amplitude of oscillation is equal to $2h$. Figure 5b presents such a solution,
– the sustained oscillation solution: the length of the heart beat period oscillates with a fixed amplitude. Figure 7 shows heart period changes in the case of such a solution. The sinus node basic oscillations with the mean period of $\langle T \rangle = 0.8$ s are modulated with the period 14, 15 beats, i.e., about 12 s. This oscillation can be identified as the Mayer wave [32]. (The exact length of the cycle is 474 heart beats in case $\theta_{cNa} = \theta_{vNa} = 3$ s.)

In a series of figures (Figs. 8, 9, 10, 11) we show the bifurcation diagrams—the heart beat periods calculated for various values of the delays. One of the sympathetic time delays (Figs. 8, 9, 10), or both of them (Fig. 11) are playing the role of the bifurcation parameter. For each value of the delays a 1,000 s record obtained from the same initial conditions is plotted. First 500 s of the transient values are omitted. The sampling step is 0.01 s.

The presented diagrams are the typical ones representing the complete bifurcation diagram which can be calculated in the whole sympathetic time delays plane $(\theta_{cNa} \times \theta_{vNa})$. The chosen values explain the possible solutions of the SH model and the bifurcation transitions. For example, let as focus on the transition shown in the bifurcation diagram in Fig. 8. It appears that (see Fig. 12):

– if $\theta_{cNa} = 1.93$ s then we obtain a fixed point (with the accuracy of the numerical method $h = 0.001$ s).
– if $\theta_{cNa} = 1.94$ s then one point solution switches into the oscillation with the period $T \approx 10$ s and the amplitude 0.003, independently of h.
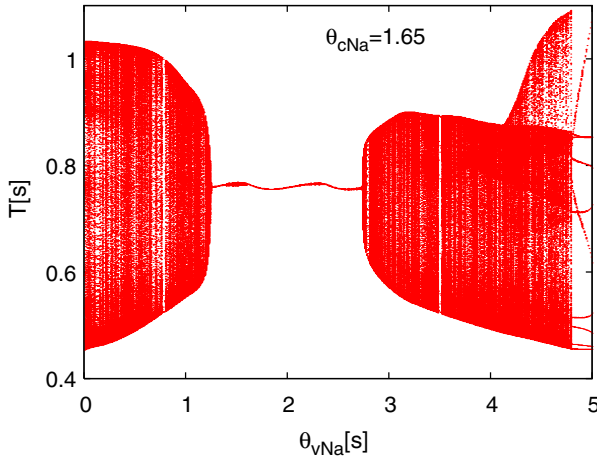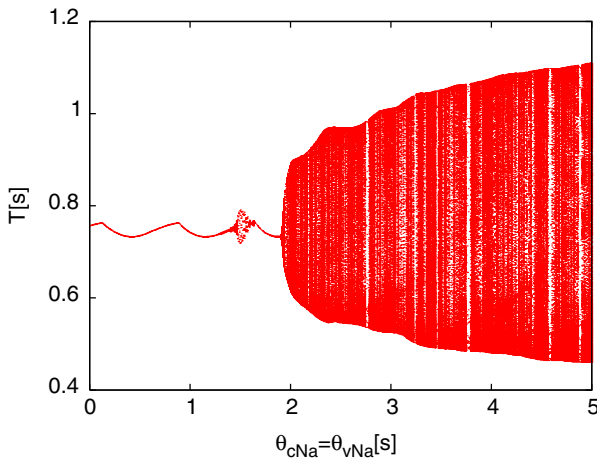
Fig. 9 Bifurcation diagram if the delay in transmitting signals from the brain to the blood vessels $\theta_{vNa} = 1.65$ s is increasing, while the delay between the brain and the heart θ_{cNa} is constant. The critical points: $\theta_{vNa} \approx 1.25$ s and $\theta_{vNa} \approx 2.74$ s. For $\theta_{vNa} > 4.79$ s one can observe the example of the island of stability
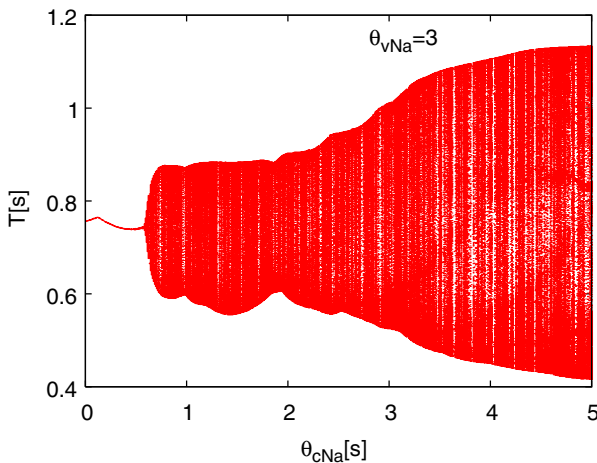
Fig. 10 Bifurcation diagram if the delay in transmitting signals from the brain to the heart θ_{cNa} is increasing, while the delay between the brain and the blood vessels is constant $\theta_{vNa} = 3$ s. The critical point $\theta_{cNa} \approx 0.58$ s

- if $\theta_{cNa} = 1.95$ s or $\theta_{cNa} = 1.96$ s then the sustained oscillation with the amplitude about 0.007 is reached, but after a significantly larger transient time.
- if $\theta_{cNa} = 1.97$ s then the ordinary sustained oscillation emerges in a time shorter then 500 s.

Hence, the bifurcation point is distinguished from the other points by the emergence of a long transient time.

Fig. 11 Bifurcation diagram if both delays in transmitting sympathetic activity from the brain to the heart θ_{cNa} and to the blood vessels θ_{vNa} are increasing accordingly

5.1 Remarks on bifurcation diagram

The phase of the sinus node ϕ without any influence of the autonomic nervous system grows linearly up to 1 within a heart period $T_0 = 1.1$ s. The two opposite mechanisms regulate the speed of ϕ growth.

The first one—the vagal activity v_p, is represented by the factor f_p in Eq. (7). Following the baroreceptor activity, the heart period is increased. If the delay in transmitting this activity to the heart is $\theta_p = 0.5$ s then the maximum of $F(\phi)$ corresponds to the maximum of $v_p(t - 0.5)$. Therefore the influence of v_p is highly effective when $\phi \approx 0.8$, what is visible in the plots of ϕ in Fig. 5.

The second one—the sympathetic activity v_s, is represented by the factor f_s in Eq. (7). If the activity of v_s is sufficiently high, then the exponential decay of the noradrenaline concentration in the heart is switching into its growth. The growing concentration of the noradrenaline c_{cNa} makes the increase of the phase ϕ faster. The next contraction of the heart occurs earlier and thus the heart period is reduced. The time delay θ_{cNa} determines the interval within each heart period when the named reduction occurs. Simultaneously, the high activity of v_s affects the vasculature—the vascular concentration of Na grows. Since the blood pressure decay constant τ_v depends on c_{vNa} then the increase of c_{vNa} makes the decay of the blood pressure faster. The delay θ_{vNa} determines the interval inside each heart period when the named faster blood pressure decay is observed.

If these both processes—the decrease in the heart period length and the increase in the blood pressure decay appear synchronously, then the consecutive heart contraction starts at the blood pressure almost equal to the pressure of the previous contraction. Also, there is no difference between the values of c_{cNa} at the beginning and the end of a heart cycle. The same goes for c_{vNa}. The model leads to the solution with a constant value of the heart period (fixed point solution). In such case a single point is
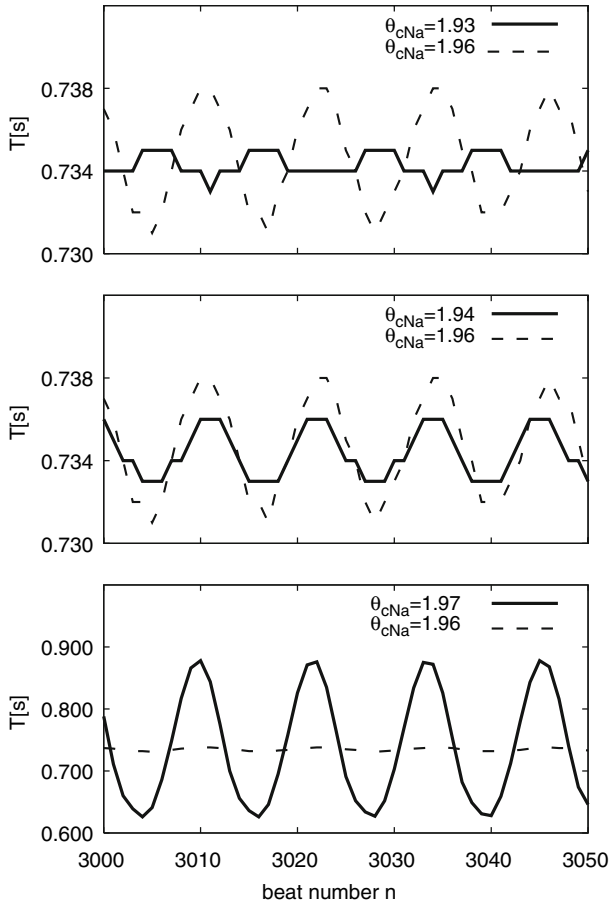
Fig. 12 The bifurcation transition with bifurcation parameter θ_{cNa}, and $\theta_{vNa} = 1.65$ s is set constant. $\theta_{cNa} = 1.93$ s—the fixed point solution (*the upper panel*), $\theta_{cNa} = 1.94$ and 1.95 s—low amplitude oscillations obtained after long transient time (*the middle panel*), $\theta_{cNa} = 1.97$ s—high amplitude oscillations revealed in less than 500 s. The solution for $\theta_{cNa} = 1.96$ s is presented for scale comparison in each case

plotted in the bifurcation diagram, see Fig. 11 for the situation with $\theta_{cNa} = \theta_{cNa} \in$ (0, 1.9) s. But a cooperation of two processes does not imply equivalence of their time scales.

When $\theta_v = \theta_c > 1.9$ s denoting that the system is adjusted to a state which took place almost three heart beats ago, the synchronization is not attained. Small numerical differences between the consecutive heart interval properties are amplified and subsequently effect (after many time steps) in the destruction of the synchronization. Properties of a system which is driven by spiky changes in the neuronal activities strongly change from one heart period to another: this is particularly visible in the case of a fragile state attained if both delays are close to the double heart period $\theta_v = \theta_c \approx 1.5$ s (see Fig. 11).

Since physiologists found that the heart rate response to the sympathetic nerve is slower than the vasculature response [9], it would be interesting to investigate the SH

model solutions in the case when the two delays are independent, compare Figs 8, 9, and 10. To this end we inspect the complete bifurcation diagram plane $(\theta_{cNa} \times \theta_{cNa})$ in the range of the parameters $[0, 5] \times [0, 5]$ s with the step 0.1 s. The rough investigation of this diagram provides four regions where a rapid switch from a fixed point solution to an oscillatory solution is observed:

I $\theta_{cNa} < 0.5$ s :

independently of the θ_{vNa} value the system limit is a fixed point solution $T^* \approx 0.75$ s. The value of the stable time period depends periodically on θ_{vNa} with a period length of about 0.75 s (See Figs. 8, 10, 11 for examples of such parameter settings.). These results suggest that the fast reaction of the cardiac noradrenaline concentration c_{cNa} to the baroreceptor stimuli provides a strong force which drives quickly to the next heart contraction, and which dominates over the other processes in the system.

II $0.5s < \theta_{cNa} < 1.0$ s:

for $\theta_{vNa} > 2.7$ s large enough the bifurcation happens. The value of θ_{vNa} at which the transition occurs depends weakly on θ_{cNa} and is approximately $\theta_{vNa} > 2.7$ s (Fig. 10 shows the example of such parameter settings).

III $1.0s < \theta_{cNa} < 2.0$ s:

apart from the region $\theta_{vNa} > 2.7$ s the oscillatory solution appears also if θ_{vNa} is small enough. Here we observe two bifurcation points: the former $\theta_{vNa}^{crit_A}$ ends the oscillatory solution region for small θ_{vNa}, while the latter $\theta_{vNa}^{crit_B}$ starts the oscillatory solution region for large θ_{vNa}. Between these two points the fixed point solution occurs. The section of the complete bifurcation diagram for a fixed $\theta_{cNa} = 1.65$ s is presented in Fig. 9. The critical points are $\theta_{vNa}^{crit_A} \approx 1.2$ s and $\theta_{vNa}^{crit_B} \approx 2.7$ s. The other critical values of θ_{cNa} in this region are presented below:

$\theta_{cNa}[s]$	1.1	1.2	1.3	1.4	1.5	1.6	1.7	1.8	1.9	2.0
$\theta_{vNa}^{crit_A}[s]$	0.4	0.5	1.1	1.3	1.5	1.3	1.3	1.3	1.5	2.2
$\theta_{vNa}^{crit_B}[s]$	2.7	2.7	2.6	2.5	2.5	2.7	2.7	2.8	2.7	2.4

In the case when $\theta_{cNa} - \theta_{vNa} > 0.5$ s then the growths of c_{cNa} and c_{vNa} are separated in time. It means that the order from the sympathetic system to speed up the blood pressure decay does not meet the elevated noradrenaline concentration c_{cNa} what accelerates the sinus node phase growth. Therefore the blood pressure at the moment of the heart contraction is lower than the blood pressure at the end of the previous diastolic phase.

IV $2.0 < \theta_{cNa}$:

for any θ_{vNa} only oscillatory solution happens.

The above presented stability analysis is rough. The bifurcation points are determined with some inaccuracy (resulted from the resolution of the diagram) and moreover the problem of the islands of stability in the oscillatory regions is completely omitted.

The vast complexity of the stability picture in this model is however beyond the basic interest of this presentation.

Closing, we should mention that the heart period length in the oscillatory solutions takes values in the interval (0.3, 1.4), what means that the heart periods vary around the fixed point solution. Moreover, it implies also that the intrinsic heart period $T_0 = 1.1$ s is shortened by the sympathetic nervous system activity to be approximately 0.8 s. One can conclude that the basic stationary state of cardiovascular system is maintained by the sympathetic system. However, if we switch off the parasympathetic influence to the sinus node phase completely (by, for instance setting $f_p = 1$) then the blood pressure and the cardiac noradrenaline concentration vary strongly, reaching unphysiological values, namely $p(t) \in (80, 200)$ mmHg and $c_{cNa} \in (0, 0.8)$ if $\theta_{vNa} = \theta_{cNa} = 3$ s. Hence the parasympathetic system influence to the stabilization is of crucial importance.

We also performed a few simulations with the sinus node intrinsic period set to $T_0 = 0.6$ s. Then the SH model provides a solution with the heart period length about 0.65 s. As it could be expected in this case, we observe a rather high value of the blood pressure, $p(t) \in (120, 160)$ mmHg what makes the baroreceptor activity really strong and results in the minimal role of the sympathetic system activity. The final effect is that the differences between the heart periods are low, namely smaller than 0.02 s.

Physiologists found that the heart rate response to the sympathetic nerve stimulation is slower than that of the vasculature [9]. With regard to the steady state changes in the sympathetic nervous activity, the heart rate response is characterized by a time delay of 1–3 s.

However, in various models the distributed delays are usually simplified and approximated with a single delay time (2–6 heart beats in DeBoer model [25], 2 s in Ursino model [30], 3 s in Fowler model [29]). Within the proposition of Seidel and Herzel we see that differentiation of delays is important since both delays actively form the solution and therefore the relation between delays deserves a special attention.

6 Stochastic approach

Noise is an intrinsic property of physiological systems [1]. Nevertheless, the deterministic models of the cardiovascular system are proposed in order to facilitate progress in its understanding. Then the noise is introduced into the model as an external perturbation to the model parameters [35]. In the case of SH model, so far it has been found that it can exhibit stable cardiorespiratory synchronization against the noise added to the baroreceptor activity [33]. Moreover, it has been also shown that thanks to the vagal activity perturbed by a gaussian white noise and baroreceptor activity perturbed by a Brownian noise, the heart rate series exhibits a long-range correlation [34]. The question that we ask in the present paper is how HRV estimated by the PDF of heartbeats changes, if the delays in transferring neural signals are perturbed by a white noise.

Let ξ be a random variable with the uniform distribution and $\xi \in [-\widehat{\xi}, \widehat{\xi}]$ for some fixed maximal level of noise $\widehat{\xi}$. Let us assume that a time, needed for a signal to transfer the neural information varies stochastically around some mean value. Then Eqs. (4) and (13) take the following form:

$$\frac{dc*}{dt} = -\frac{c*}{\tau*} + k_*^s v_s (t - (\theta_* + \xi_*))$$
(16)

where * represents parameters related either to heart cNa or to vasculature vNa. The random numbers are generated by standard 48-bit arithmetic functions accessible in C compilers in Unix systems.

Na concentration acts like a buffer, so the distribution of the sympathetic impulses over a heart cycle is not very important [32]. Moreover, Na needs to be removed
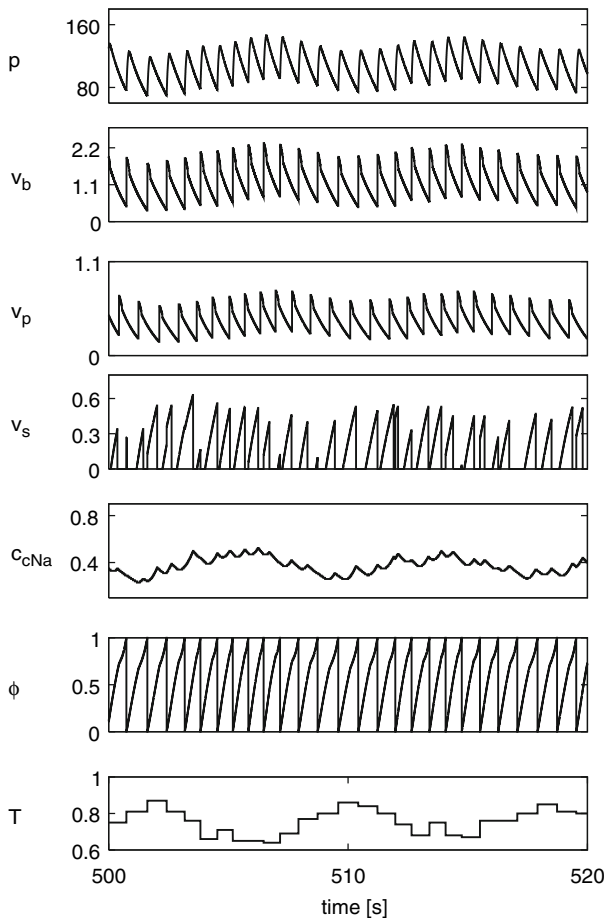
Fig. 13 Time series obtained by simulating the model with stochastic delays—the case of the fixed point solution stochastically perturbed, $\theta_{vNa} = \theta_{vNa} = 1.65$, the noise level: $\widehat{\xi} = 1$ s. See Fig. 5 for detailed description of y axis
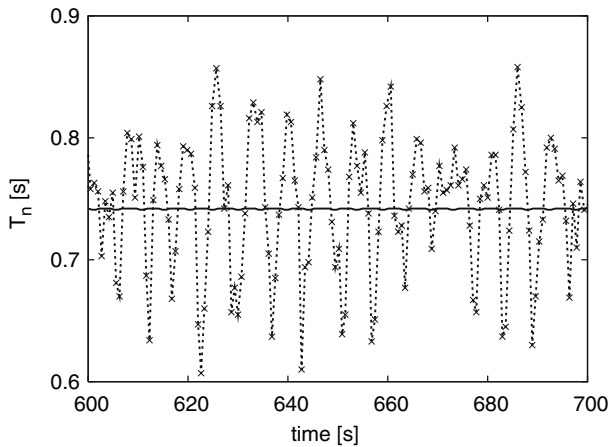
Fig. 14 Time series of T obtained in deterministic case when $\theta_{cNa} = \theta_{vNa} = 1$ (the fixed point solution) and with delays stochastically perturbed with $\widehat{\xi} = 0.5$

from the synaptic gap and delivered down to a different location. This process takes much more time than a time step of the model simulation. Therefore we assign a new random value to each delay for each cardiac cycle separately. To avoid effects related to respiration we again consider the system with the constant respiration only.

One can as well model the noise ξ_* by a continuous variable. In this case, at each numerical step the delay is set to a different random value. It appears that such randomness of delays does not cause significant change in the solutions.

### 6.1 Stochastic perturbation to a fixed point heart rate

If the time delays are stochastic then even in the absence of the respiration the stable heart rate becomes irregular. Figure 13 shows the time series obtained when the values of delays are taken independently and uniformly from the interval $[0.65, 2.65]$ s . The regular waveforms obtained in the deterministic case (compare to Fig. 5b) are now varying irregularly, Fig. 14. The unperturbed evolution provides the histogram of the heart beat periods (the histogram bin is equal to 0.01) with one peak, see Fig. 15a. Depending on the magnitude of the added noise this line becomes broadened. Note that even at the low level of the noise, namely if $\widehat{\xi} \geq 0.1$, the histogram shape resembles the distribution of the real-life series of NN intervals presented in Fig. 1. Moreover, the Poincaré plot of the solution with the noise level $\widehat{\xi} = 1$ s (Fig. 16) resembles the diagrams for NN series (see Fig. 2).

6.2 Stochastic perturbation to an oscillating heart rate

In the case when $\theta_{cNa} = \theta_{vNa} = 3$ s the deterministic SH model provides the sustained 10 s rhythms, see Fig. 7. Figure 17 shows an example of the series obtained when delays are random and large $2s < \theta_{cNa}, \theta_{vNa} < 4$ s.
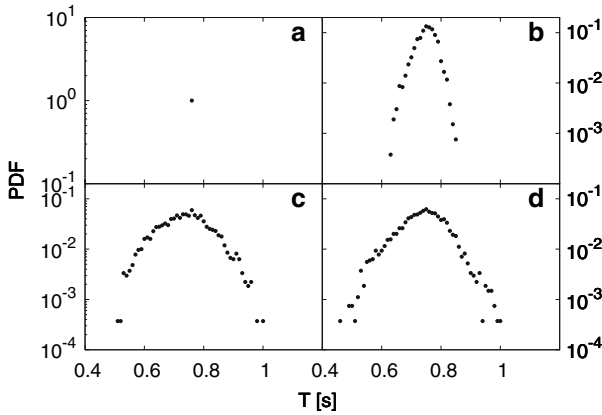
Fig. 15 PDF of the heart beat period T in case of the fixed point solution. The unperturbed evolution (**a**) and the evolution with the increasing level of noise is shown in subsequent panels (**b–d**). The log scale is applied to PDF axis. $\theta_{vNa} = \theta_{vNa} = 1.65\,\text{s}$, the noise level: **a** $\widehat{\xi} = 0$, **b** $\widehat{\xi} = 0.1\,\text{s}$, **c** $\widehat{\xi} = 0.5\,\text{s}$, **d** $\widehat{\xi} = 1\,\text{s}$
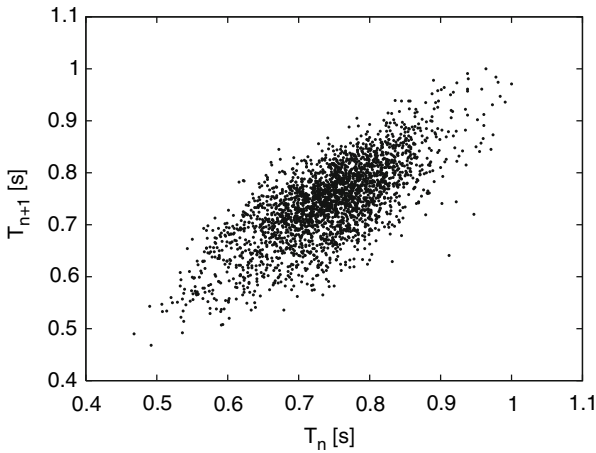

Fig. 16 Poincaré plot for fixed point solution ($\theta_{vNa} = \theta_{vNa} = 1.65\,\text{s}$) perturbed by noise of level $\widehat{\xi} = 1\,\text{s}$. The PDF of this series is presented in Fig. 15d

The histogram of the heart beat intervals in the case of the deterministic dynamics takes the form of a double peaked distribution with two sharp peaks at the left and the right wing, see Fig. 18a. The shortest and the longest period appear with the probability ten times larger than the mean value. Such a distribution does not resemble any distribution found for the real-life NN interval series.

The stochastic noise makes the modeled distribution of the heart beat periods similar to the real-life data distribution. When the noise level is large enough the distribution almost approaches the desired shape, see Fig. 18d.

What is important is that the main oscillation of the deterministic solution (i.e., the Mayer wave) is preserved, see Fig. 19, and additionally, the return plot for the heart beat series resembles the plots known for the real-life time series (see Fig. 2).
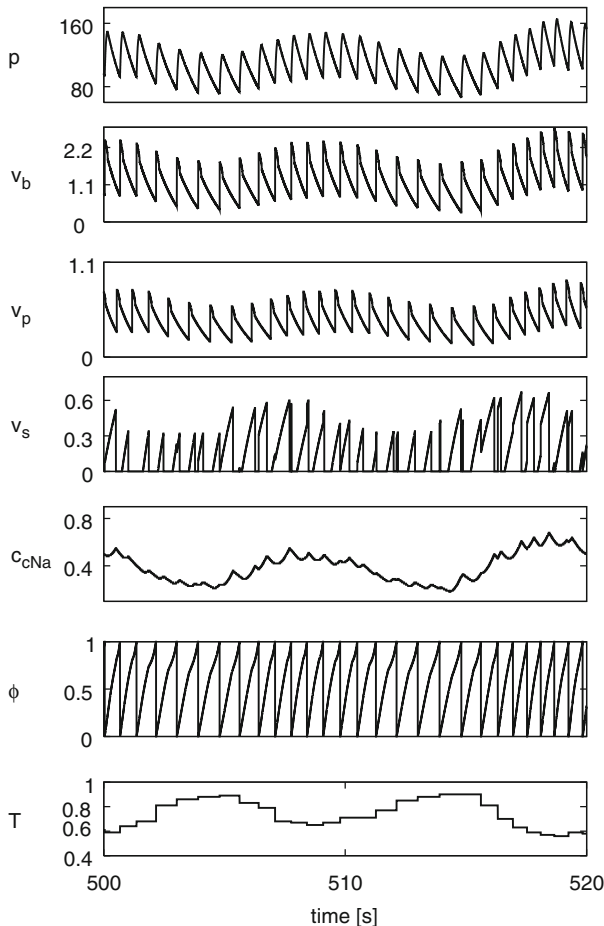
Fig. 17 Time series obtained by simulating the model with stochastic delays—the case of the sustained oscillation of heart period stochastically perturbed. $\theta_{vNa} = \theta_{vNa} = 3\,\mathrm{s}$, $\widehat{\xi} = 1\,\mathrm{s}$ Sympathetic time delays are taken independently and uniformly from the interval $[2, 4]\,\mathrm{s}$. See Fig. 5 for detailed description of y axis

Notably, the overall shape of this plot seems to be inherited from the deterministic solution (see Fig. 7), although the inside of the limit cycle is now densely occupied.

6.3 The effect of noise on stability

The bifurcation diagram smooths out when the noise is added to the delays. Critical points disappear, namely there is no rapid change in the type of the solution when the mean delay changes. The intervals of the stable point solutions become regions of the sustained oscillations with a slightly smaller amplitude than the amplitude of the oscillations arisen after the bifurcation, see Figs. 20 and 21. Let us notice that at the
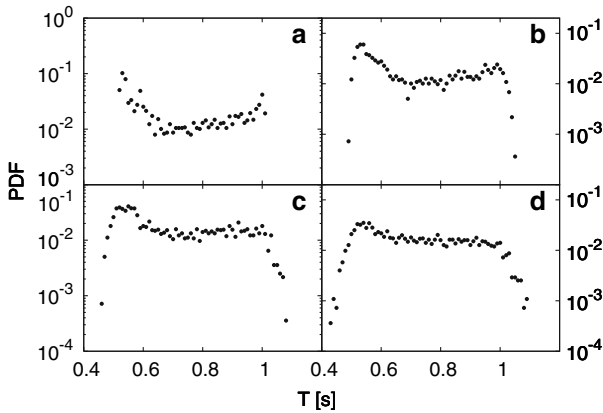
Fig. 18 PDF of the heart period T in case oscillating heart rate. The unperturbed evolution (**a**) and evolution with the increasing level of noise is shown in subsequent panels (**b**–**d**). The log scale is applied to PDF axis. $\theta_{vNa} = \theta_{vNa} = 3$ s, noise level **a** $\widehat{\xi} = 0$, **b** $\widehat{\xi} = 0.5$ s, **c** $\widehat{\xi} = 1$ s, **d** $\widehat{\xi} = 1.5$ s

noise level $\widehat{\xi} = 0.5$ the spread of the heart beat intervals is larger than 0.2 s, even in the stable region of the deterministic solution. Moreover, Mayer wave type oscillations are present, see Fig. 14, even far away from the deterministic bifurcation point.

7 Conclusion

Models of the cardiovascular interactions are still debated [9,10]: one is faced with a rather broad range of possible parametric models to consider [25–27,29,30]. In this paper we investigated the statistical and dynamical properties of the SH nonlinear model of baroreflex—the scheme that is assumed to provide a short-term control of the cardiorespiratory system. SH model is sufficiently simple to allow a mathematical analysis of dynamics and at the same time sufficiently complete to provide a faithful representation of the underlying physiology. The model is capable (after Kotani et al. modification [33]) to describe the interactions between the three main rhythms of the human physiology: the heart rate, the blood pressure and the respiration. Hence, it is an appropriate proposition for investigations of reasons of HRV. The sustained oscillations in the heart rate and blood pressure interpreted as the Mayer waves emerge here as the resonance effect between intrinsic oscillations and delays, when varying the delay parameters.

When sympathetic time delays are perturbed by a white noise, the statistical features of the real-life cardiorespiratory system, such as the probability density functions of NN intervals, and geometrical properties of return plots of NN intervals are resembled. Moreover, in the case of the stochastic model the bifurcation points vanish and the Mayer oscillations in the heart period and the blood pressure are observed for the whole considered space of the sympathetic time delays.

When dealing with the loop dependencies one could expect that the stochastic perturbation of any parameter will effect the solution in a similar way. However, here in the SH model, if the time delays are considered as random we obtain a possibility
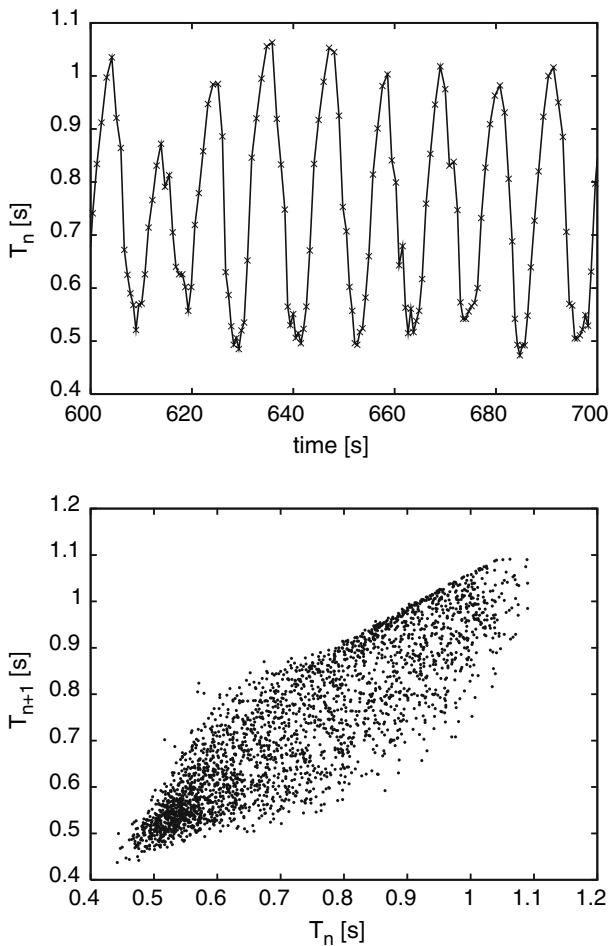
Fig. 19 Time series of heart periods T in case of the sustained oscillation solution for the random delays. $\theta_{vNa} = \theta_{vNa} = 3$ s, noise level $\widehat{\xi} = 1$ s. Notice that low frequency oscillations are preserved, though they appear with different amplitudes, what results that the return plot is the cloud of points

to separate two physiological processes driving the blood pressure. The concentration of the noradrenaline in vasculature determines the diastolic blood pressure while the concentration of the noradrenaline in the heart via change in the cardiac contractility determines the systolic blood pressure. Therefore, the activity of baroreceptors as well as the sympathetic nerves activity contains both effects. For this reason their stochastic properties are different from those when a simple white noise is added to them. What is to be discussed is the type of the randomness that is inserted into the time delays. For simplicity we considered a white noise although any noise in the biological systems usually exhibit $1/f$ type power spectrum, what is opposed to a white noise which has a flat power spectrum. Moreover, it has been found experimentally [43] that $1/f$ noise added externally to the baroreflex centers via venous blood pressure receptors affects the heart rate response more strongly than the white noise. The investigations
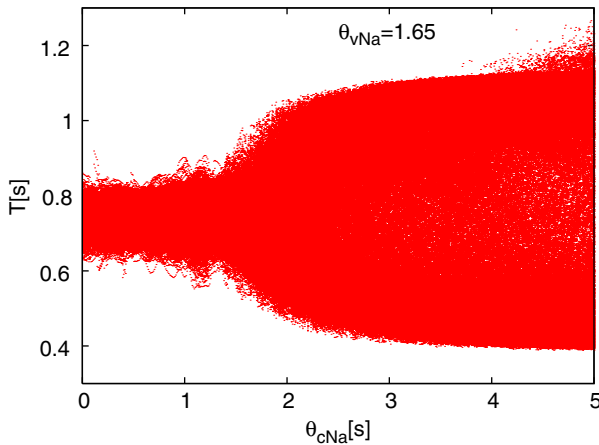
Fig. 20 Diagram of heart beat periods if the delay in transmitting signals from the brain to the heart θ_{cNa} is increasing, while the delay between the brain and the blood vessels is constant $\theta_{vNa} = 1.65$ s. Both delays change stochastically in each heart beat interval, noise level $\widehat{\xi} = 0.5$
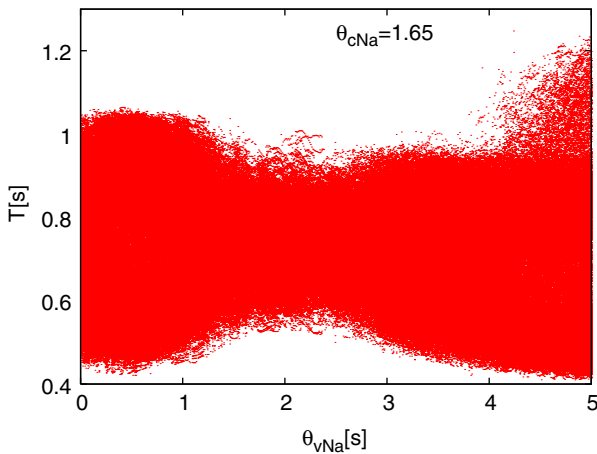
Fig. 21 Diagram of heart beat periods if the delay in transmitting signals from the brain to the blood vessels θ_{vNa} is increasing, while the delay between the brain and the heart is constant $\theta_{cNa} = 1.65$ s. Both delays change stochastically in each heart beat interval, noise level $\widehat{\xi} = 0.5$

regarding the differences in the influence related to various noise types we leave for the further studies.

In the further investigations the time delay of the vagally cardiac baroreflex response should be considered as varying also since it is known that this time delay is influenced by the postural changes and/or can be changed by the introduction of the atropine [44].

References

1. Glass, L.: Synchronization and rhythmic processes in physiology. Nature **410**, 277 (2001)
2. Peng, C.K., Mietus, J., Hausdorff, J.M., Havlin, S., Stanley, H.E., Goldberger, A.L.: Long-range anticorrelations and non-gaussian behavior of the heartbeat. Phys. Rev. Lett. **70**, 1343 (1993)
3. Yamamoto, Y., Hughson, R.L.: On the fractal nature of heart rate variability in humans: effects of data length and β-adrenergic blockade. Am. J. Physiol. **266**, R40 (1994)
4. Ivanov, P.C., Amaral, L.A.N., Goldberger, A.L., Havlin, S., Rosenblum, M.G., Struzik, Z.R., Stanley, H.E.: Multifractality in human heart rate dynamics. Nature **399**, 461 (1999)
5. Makowiec, D., Gałąska, R., Dudkowska, A., Rynkiewicz, A., Zwierz, M.: Long-range dependencies in heart rate signals—revisited. Physica A **369**(2), 632 (2006)
6. Kiyono, K., Struzik, Z.R., Aoyagi, N., Togo, F., Yamamoto, Y.: Phase transition in a healthy human heart rate. Phys. Rev. Lett. **95**, 058101 (2005)
7. Heart rate variability. Standards of measurment, physiological interpretation, and clinical use. Eur. Heart J. **17**, 354 (1996)
8. Malik, M.: Heart Rate Variability and Baroreflex Sensitivity in Cardiac Electrophysiology. In: Zipes, D.P., Jalife, J. (eds.) From Cell To Bedside, 4th edn, Saunders, Philadelphia (2004)
9. Malpas, S.C.: Neural influences on cardiovascular variability: possibilities and pitfalls. Am. J. Physiol. Heart Circ. Physiol. **282**, H6 (2002)
10. Julien, C.: The enigma of Mayer waves: facts and models. Cardiovasc. Res. **70**, 12 (2006)
11. Eckberg, D.L., Sleight, P.: Human Baroreflexes in Health and Disease. Clarendon Press, Oxford (1992)
12. Bertram, D., Barre's, C., Cheng, Y., Julien, C.: Norepinephrine reuptake, baroreflex dynamics, and arterial pressure variability in rats. Am. J. Physiol. Regul. Integr. Comp. Physiol. **279**, R1257 (2000)
13. Pikovsky, A., Rosenblum, M., Kurths, J.: Phase synchronization in regular and chaotic systems. Int. J. Bif. Chaos **10**, 2291 (2000)
14. Schäfer, C.S., Rosenblum, M.G., Kurths, J., Abel, H.: Heartbeat synchronized with ventilation. Nature **392**, 239 (1998)
15. Lotrič, M.B., Stefanovska, A.: Synchronization and modulation in the human cardiorespiratory system. Physica A **283**, 451 (2000)
16. Prokhorov, M.D., Ponomarenko, V.I., Gridnev, V.I., Bodrov, M.B., Bespyatov, A.B.: Synchronization between main rhythmic processes in the human cardiovascular system. Phys. Rev. E **68**, 041913 (2003)
17. Stefanovska, A., Haken, H., McClintock, P.V.E., Hožič, M., Bajrović, F., Ribarič, S.: Reversible transitions between synchronization states of the cardiorespiratory system. Phys. Rev. Lett. **85**, 4831 (2000)
18. Censi, F., Calcagnini, G., Cerutti, S.: Coupling patterns between spontaneous rhythms and respiration in cardiovascular variability signals. Comput. Methods Programs Biomed. **68**, 37 (2002)
19. Rosenblum, M.G., Cimponeriu, L., Bezerianos, A., Patzak, A., Mrowka, R.: Identification of coupling direction: application to cardiorespiratory interaction. Phys. Rev. E **65**, 041909 (2002)
20. Smirnov, D.A., Bezruchko, B.P.: Estimation of interaction strength and direction from short and noisy time series. Phys. Rev. E **68**, 046209 (2003)
21. Ponomarenko, V.I., Prokhorov, M.D., Bespyatov, A.B., Bodrov, M.B., Gridnev, V.I.: Deriving main rhythms of the human cardiovascular system from the heartbeat time series and detecting their synchronization. Chaos Solitons Fractals **23**, 1429 (2005)
22. Schäfer, C., Rosenblum, M.G., Abel, H.H., Kurths, J.: Synchronization in the human cardiorespiratory system. Phys. Rev. E **60**, 857 (1999)
23. Prokhorov, M.D., Ponomarenko, V.I.: Estimation of coupling between time-delay systems from time series. Phys. Rev. E **72**, 016210 (2005)
24. Smelyanskiy, V.N., Luchinsky, D.G., Stefanovska, A., McClintock, P.V.E.: Inference of a nonlinear stochastic model of the cardiorespiratory interaction. Phys. Rev. Lett. **94**, 098101 (2005)
25. DeBoer, R.W., Karemaker, J.M., Strackee, J.: Hemodynamic fluctuations and baroreflex sensitivity in humans: a beat-to-beat model. Am. J. Physiol. **253**, 680 (1987)
26. Abbiw-Jackson, R.M., Langford, W.F.: Gain-induced oscillations in blood pressure. J. Math. Biol. **37**, 203 (1998)
27. Eyal, S., Akselrod, S.: Bifurcation in a simple model of the cardiovascular system. Method. Inform. Med. **39**, 118 (2000)
28. Ottesen, J.T.: Modelling of the baroreflex-feedback mechanism with time-delay. J. Math. Biol. **36**, 41 (1997)

29. Fowler, A.C., McGuinness, M.J.: A delay recruitment model of the cardiovascular control system. J. Math. Biol. **51**, 508 (2005)
30. Magosso, E., Biavati, V., Ursino, M.: Role of the Baroreflex in Cardiovascular Instability: A Modeling Study. Cardiov. Eng. **1**(2), 101 (2001)
31. Seidel, H., Herzel, H.: Bifurcations in a nonlinear model of the baroreceptor-cardiac reflex. Physica D **115**, 145 (1998)
32. Seidel, H., Herzel, H.: Modeling heart rate variability due to respiration and baroreflex. In: Mosekilde, E., Mouritsen, O.G. (eds.) Modeling the Dynamics of Biological Systems., pp. 205–229. Springer, Berlin (1995)
33. Kotani, K., Takamasu, K., Ashkenazy, Y., Stanley, H.E., Yamamoto, Y.: Model for cardiorespiratory synchronization in humans. Phys. Rev. E **65**, 051923 (2002)
34. Kotani, K., Struzik, Z.R., Takamasu, K., Stanley, H.E., Yamamoto, Y.: Model for complex heart rate dynamics in health and diseases. Phys. Rev. E **72**, 041904 (2005)
35. Ruelle, D.: Where can one hope to profitably apply the ideas of chaos?. Phys. Today **47**, 29 (1994)
36. Mc Clintock, P.V.E., Stefanovska, A.: Noise and determinism in cardiovascular dynamics. Physica A **314**, 69 (2002)
37. Woo, M.A., Stevenson, W.G., Moser, D.K., Trelease, R.B., Harper, R.M.: Patterns of beat-to-beat heart rate variability in advanced heart failure. Am. Heart J. **123**, 704 (1992)
38. The NN series collected and selected in Medical Academy of Gdańsk analysed in [5], http://iftia9. univ.gda.pl/~danka/DATA/
39. Keener, J.P., Hoppensteadt, F.C., Rinzel, F.C.: Integrate and fire models of nerve membrane response to oscillatory input. SIAM J. Appl. Math. **41**, 127 (1981)
40. Press, W.H., Teukolsky, S.A., Vetterling, W.T., Flannery, B.P.: Numerical Recipes in C. Cambridge University Press, Cambridge (1992)
41. Farmer, J.D.: Chaotic attractors of an infinite-dimensional dynamic systems. Physica D **4**, 366 (1982)
42. Glass, L., Malta, C.P.: Chaos in multi-looped negative feedback system. J. Theor. Biol. **145**, 217 (1990)
43. Soma, R., Nozaki, D., Kwak, S., Yamamoto, Y.: 1/f Noise outperforms white noise in sensitizing baroreflex function in the human brain. Phys. Rev. Lett. **91**, 078101 (2003)
44. Keyl, C., Schneider, A., Dambacher, M., Bernardi, L.: Time delay of vagally mediated cardiac baroreflex response varies with autonomic cardiovascular control. J. Appl. Physiol. **91**, 283 (2001)